



Computational Development of New Inhibitors for Apoptosis-Stimulating Protein of p53 (iASPP) Using Pharmacophore Modeling, Docking, and MD Simulation Approaches

Aftab Alam¹, Muhammad Junaid², Muhammad Fawad Ali¹, Sajid Ali³, Muhammad Riaz⁴, Sana Haq⁵, Abdul Wadood^{1,*}

¹Department of Biochemistry, Abdul Wali Khan University, Mardan, Mardan, 23200, Pakistan.

²Department of Bioinformatics, Shanghai Jiao Tong University, Shanghai, China.

³Department of Chemistry, Bacha Khan University, Charsadda, Pakistan.

⁴Government Degree College Garhi Kapura, Mardan, KPK, Pakistan.

⁵Sardar Begum Dental Hospital, Gandhara, University of Peshawar, Pakistan.

*Corresponding author: Abdul Wadood, awadood@awkum.edu.pk

Article history

Received: 30 July 2024

Revised: 18 September 2024

Accepted: 20 September 2024

Published online: 9 October 2024

Keywords

Pharmacophore Model

Validation

Molecular Docking

Molecular Dynamics Simulation

Abstract

Inhibitor of apoptosis-stimulating protein of p53 (iASPP) overexpression is associated with diverse human tumors, including lung cancer, colorectal cancer, prostate cancer, acute leukemia, hepatocellular carcinoma, cervical cancer, and ovarian cancer. This study aims to find new and potent inhibitors for the iASPP drug target. Using pharmacophore-based virtual screening, molecular docking, and molecular dynamics simulation an integrated strategy was developed to find highly effective iASPP inhibitors. Subsequently, the pharmacophore model was employed as a screening query to find promising inhibitors from the ZINC database. Total 36/12000 hits were identified against the iASPP drug target. The binding mode of the promising identified inhibitors was predicted by a molecular docking study. To evaluate the stability of the newly identified inhibitors top 03 best docking scores compounds were subjected to MD simulation. MD simulation and binding energy calculation confirmed that the compounds including ZINC001361049159, ZINC001361124195, and ZINC001545869876 were stable. The MD simulation analysis indicated that among all the compounds ZINC001361049159 was the most potent. These newly designed iASPP inhibitors could be used as starting material to identify new and potent anti-cancer drugs.

1. Introduction

One of the leading causes of cancer-related death globally is considered to be lung cancer [1]. Despite the increased focus on preventive healthcare, an estimated 1.8 million new instances of lung cancer are diagnosed each year, with non-small cell lung cancer (NSCLC) accounting for the most of these cases. Target treatments are improving lung cancer patients' clinical results, but drug resistance is a major problem [2]. New treatments are therefore required. Cell division, an essential process that enables cells to proliferate, replicate their DNA, and divide, is generally altered in cancer. Signaling pathways that include numerous regulators, including p53, often regulate the cell cycle. The P53 gene function in preserving stability by ensuring that replication errors are fixed, this regulator may defend the genome [3]. As a result, p53 deregulation could prevent cell cycle arrest, apoptosis, senescence, and autophagy. According to a number of studies, the binding of MDM2 and subsequent induction of p53 proteasome degradation inhibits the activity of p53. Additionally, the majority of malignancies have been found to have a high p53 mutation rate [4]. The mutant p53 may develop

carcinogenic activities by interfering with its downstream gene expressions [5].

P53 is involved in the control of the epithelial-to-mesenchymal transition and the features of cancer stem cells in addition to cell proliferation [6]. Therefore, restoring wild-type p53 function may pave the way for the treatment of cancer. Increasing evidence demonstrates that the PPP1R13L gene, which encodes iASPP protein overexpression is linked to malignancies [7]. ASPP1, ASPP2 and iASPP are the members of the p53 family of proteins. The first two serve as typical p53 activators whereas iASPP functions as an inhibitor that can directly reduce the apoptotic transactivation potential of p53. iASPP can also stimulate p53-independent carcinogenesis and suppress the apoptotic activities of p63 and p73 [8]. iASPP is considered to promote carcinogenesis through p53-independent mechanisms, primarily by preventing p63 and p73 from triggering apoptosis. Notably, iASPP can induce apoptosis in healthy cells by inhibiting nuclear factor-B (NF-B). iASPP overexpression is associated with diverse human tumors, such as lung cancer, colon cancer, prostate cancer, acute leukemia, head and neck carcinoma, hepatocellular carcinoma, and ovarian cancer [9]. iASPP

can be broadly classified into 2 isoforms, each of which has 407 and 828 amino acids. A potential strategy for regaining p53 function could be possible by focusing on and targeting iASPP [10].

Developing a new drug is costly, and time-consuming and the estimated cost ranging from \$314 million to \$2.8 billion [11]. Therefore, new strategies are required to address these financial and time-related issues. Modern drug discovery relies extensively on computer-aided drug design (CADD), which has grown into a key tool for the pharmaceutical industry. Structure and ligand-based drug design (LBDD) are two broad categories of CADD. LBDD is usually preferred if the 3D structure of the target is unknown [12]. Nowadays, pharmacophore-modeling is consistently used in medicinal chemistry labs [13]. By using a common feature-based alignment, it can more precisely and quickly find new and potent inhibitors against the drug targets [14]. In this study, the X-ray crystallographic structure of the iASPP was used to build a pharmacophore model. A number of iASPP inhibitors were successfully identified by *in silico* approaches.

2. Method

Figure 1 shows the workflow of the study carried out for new inhibitors identification.

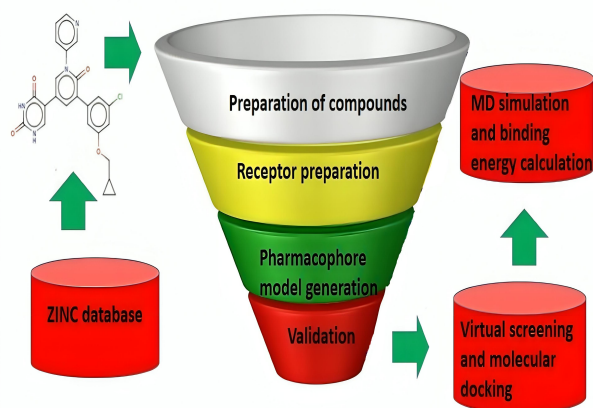


Figure 1. Systematic workflow describing the computational identification of new inhibitors for iASPP drug target.

2.1 Pharmacophore Model Generation and Evaluation

The X-ray structure of iASPP retrieved from the PDB database (PDB ID: 6RZ3) [15] was used for pharmacophore model generation. The most representative feature pharmacophore model of the iASPP active site which made interaction with the ligand was developed by using the Molecular Operating Environment (MOE) pharmacophore generation protocol [16]. The pharmacophore model was evaluated by the GH score method [17]. A database of 600 compounds was developed with 100 active compounds while the remaining compounds were inactive. The database was utilized to assess the pharmacophore model's capacity to discriminate between active and inactive compounds.

Using the MOE-available pharmacophore search procedure, the database screening was carried out. To validate the developed pharmacophore model the goodness-of-hit score (GH) was applied. The null and ideal models can be indicated by 0 and 1 GH scores respectively [18].

2.2 Docking Study

The 3D structure of iASPP (PDB code: 6RZ3) was downloaded from the PDB database. In order to add hydrogen atoms to the receptor 3D protonation was carried out [19,20]. Energy minimization was carried out for all the ligands as well as the receptor and the receptor. Compounds in lowest energy form were further processed [19]. Further, 12000 compounds were retrieved from the ZINC database. Molecular docking methods can be used to predict ligands and receptor interactions. MOE site finder option was used to predict the active site. Five conformers in total were generated for each compound and docking was performed using GBVI/WSA score function [21,22].

2.3 MD Simulation

Molecular dynamics simulations were run with the help of the AMBER 22 package [23]. The FF14SB was employed as the protein force field while the GAFF was used for the ligands [24]. At a distance of 10 Å, complexes were soaked in a TIP3P water box. The complex charge was neutralized by introducing the appropriate number of sodium ions [25]. Long-range electrostatic interactions were handled by the particle mesh Ewald (PME) during the simulation [26]. Then 5000 steps of the steepest descent and 10000 steps of conjugate gradient were applied for energy minimization. The systems were then each slowly heated from 0 to 300 K [21,30]. All the systems were then equilibrated and the 100 ns production process was run under constant temperature and pressure. Finally, trajectory analysis was performed using the CPPTRAJ [27].

2.4 MMGBSA Analysis

The MMGBSA approach was applied to estimate the binding free energy between ligands and protein complexes [23]. For binding free energy calculation the last 500 frames were used. The free energy calculation was performed using the following equation.

$$G_{bind} = \Delta G_{complex} - [\Delta G_{receptor} + \Delta G_{ligand}]$$

3. Results

3.1 Pharmacophore Model Generation

A five features pharmacophore model was developed including three hydrogen bond acceptors, one hydrophobic, and one Don and Acc. Consequently, these features may be regarded as crucial in the search for new iASPP inhibitors. Figure 2 illustrates the pharmacophore model developed in MOE software. Before using, the pharmacophore model for virtual screening the model was validated by the GH score.

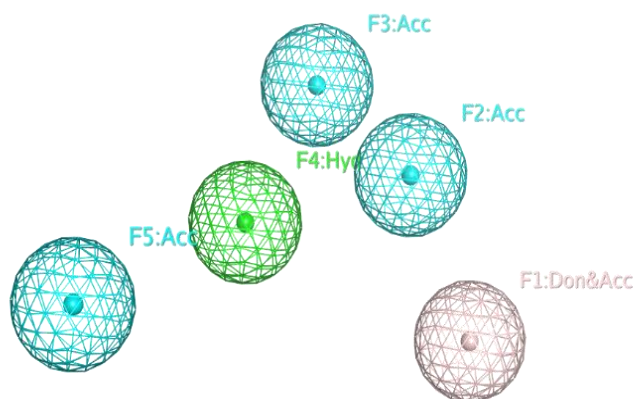


Figure 2. The generated pharmacophore model in MOE software. Pharmacophore features are color-coded, Pink (F1: Don, Acc), Cyan (F2, F3, F5 acceptor), and green (F4: Hyd).

3.2 Model Validation and Database Screening

To validate the pharmacophore model, an internal database was prepared that contains the active compounds and the decoys. The internal database contains 100 active compounds for the iASPP drug target retrieved from the Binding databank database while 500 decoys (inactive) are generated by the DUDE database. The pharmacophore model was utilized to conduct an internal database screening to evaluate the model's discriminating power. Table 1 presents the results of the calculation of several important metrics, of model validation. A model is considered validated when its GH score is greater than 0.7. It was found to be 0.85 for our model, suggesting that the pharmacophore model performed well in differentiating between active and inactive compounds. The validated pharmacophore model was employed for the virtual screening of ZINC database to find promising molecules against the iASPP drug target. A total of 36\12000 compounds were found as active by the pharmacophore model

Table 1. Pharmacophore model validation by the GH scoring method

S. No	Parameters	Outcome
1	Total compounds in internal database (D)	600
2	Total active compounds in internal database (A)	100
3	Total hits (Ht)	68
4	Active hits (Ha)	64
5	% Yield of actives ((Ha/Ht) *100)	94
6	% Ratio of actives ((Ha/A) *100)	64
7	Enrichment factor (E) ((Ha *D)/(Ht * A))	6
8	GH score	0.85

3.3 Molecular Docking Analysis

All 36 active hits were docked against the iASPP receptor. All the compounds accommodate well into the active site of the iASPP drug target. Out of 36 active hits, ZINC001361049159 was predicted potent with an S score of -7.12Kcal/mol. The compound ZINC001361049159 established four hydrogen bonds with GLN753, ASP791, GLU752, two hydrogen bonds with ARG790, and TRP799, and one Pi-H interaction with THR 722 residues. ZINC001361124195 revealed an S score of -6.13 and made five bonds with the binding site of the receptor. The compound ZINC001361124195 made two hydrogen bonds with ASP791, GLN753, one

hydrogen bond with ARG812. The compound formed one Pi-H contact with Pro793 and one pi-cation bond with Arg812 amino acid of the receptor. The S score of ligand ZINC001545869876 was predicted as -6.10. The hit ZINC001545869876 established two H-donor, one H-acceptor and two Pi-H contacts with ASP797, GLU752, THR796 and Asp791 active site residues respectively. Table 2 describes the residues involved in interaction for the 12 best hits. For docking study, NSC59984 was taken as the control compound [28]. The three-dimensional interactions of the three best-docked compounds along with the control compound are illustrated in Figure 3. Table 3 shows the 2D structures of the most potent compounds.

Table 2. The docking score and residues involved in interaction for the top 12 best docking scores compounds of the ZINC database.

ZINC ID	Interacting residues	Docking score Kcal/mol
ZINC001361124195	ASP791, GLN753, ARG812, PRO793	-6.13
ZINC001361049159	GLN753, ASP791, GLU752, ARG790, TRP799, THR722	-7.12
ZINC001545869876	ASP797, GLU752, THR796, ASP791	-6.10
ZINC000015004077	ARG812, PRO793, THR796	-4.93
ZINC001359890400	GLU732, PHE720, TRP799, ARG812	-5.64
ZINC001361126467	GLN753, ASP791, GLN753, ARG812	-5.63
ZINC001361180919	GLU752, ARG812, PHE731, PHE720	-6.03
ZINC001492607841	GLU752, PHE731, ARG812	-6.13
ZINC001545866071	PHE720, GLU752, THR796	-5.64
ZINC001360049822	ASP797, PHE720, ARG812, THR729	-5.60
ZINC000245280751	GLU752, GLU732, ARG812	-5.86
ZINC001360448324	ASP791, THR796, ARG790	-5.12
NSC59984	GLU752, ARG790, TRP788	-5.10

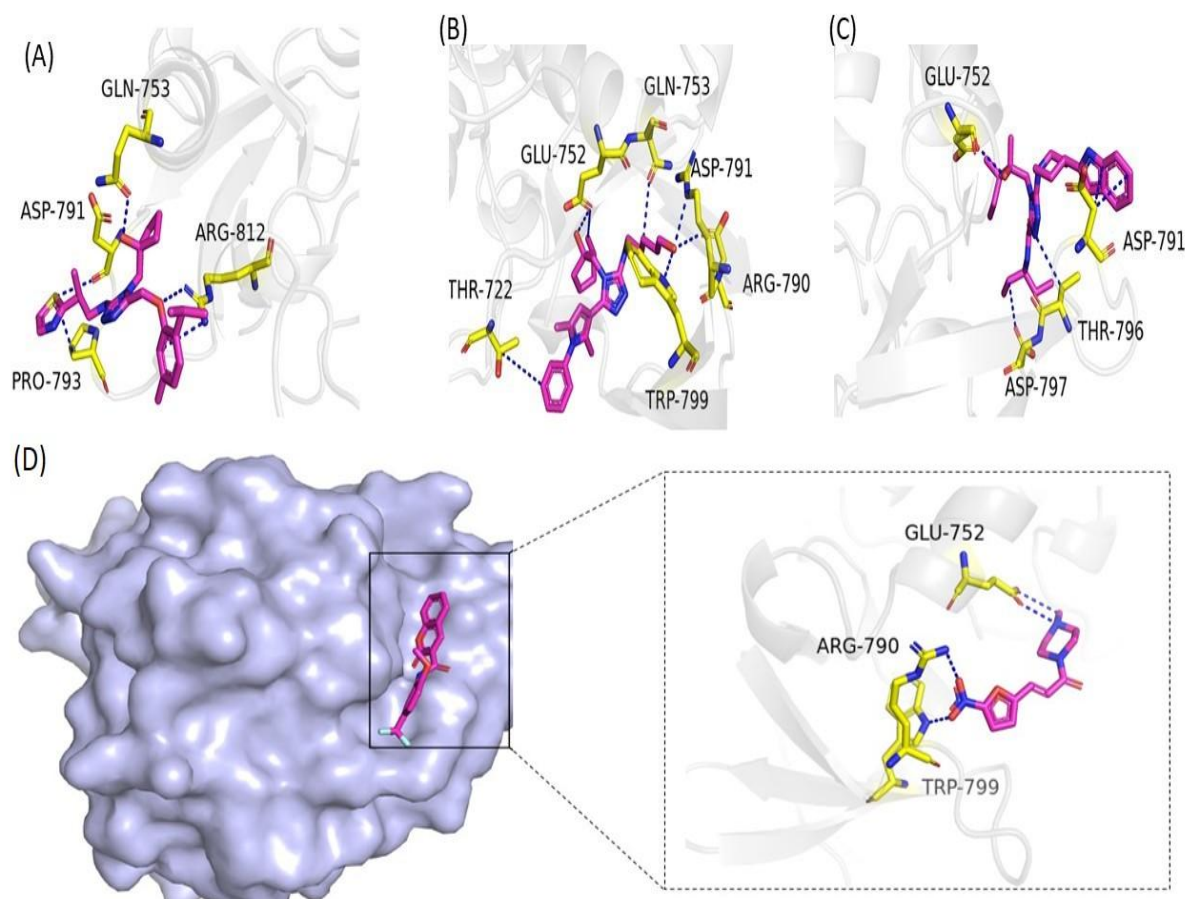


Figure 3. 3D interactions of (A) ZINC001361124195, (B) ZINC001361049159 and (C) ZINC001545869876, and (D) control compound with the iASPP drug target. The blue dash line indicates the bonds; the yellow sticks indicate the active site residues of the iASPP.

Table 3. 2D structures of the most potent compounds as well as the reference compound

Compound ID	2D structures
ZINC001361124195	
ZINC001361049159	
ZINC001545869876	
Control (NSC59984)	

3.4 Post Simulation Analysis

3.4.1 Stability of Protein-Ligand Complexes

By analyzing the RMSD, the dynamic stability and structural changes were investigated [29]. The molecular dynamics simulation results showed that the ZINC001361049159-iASPP complex reached equilibration at a time of 21 ns and that the system was observed to be stable for up to 21 ns (Figure 4). However, fluctuations were observed from 21-42ns then system converged and remained stable till 100ns MD simulation. The RMSD of the ZINC001361124195-iASPP complex was stable during the first 18ns after that deviations were observed till 50ns however, after 50ns the complex revealed stability and persisted stable till 100ns. The RMSD analysis shows that the ZINC001545869876-iASPP complex was stable during the first 5ns after that, major deviations were detected and the system revealed unstable behavior till 50ns after that the RMSD converged and the system achieved consistent stability till the end of the simulation. As compared to all other systems the RMSD of the Apo system was very high and the system revealed unstable behavior till 45ns then the system revealed stability till 100ns. As compared to all other systems the RMSD was found to be highly stable for the ZINC001361049159-iASPP system. In comparison to the control system the RMSD plot for all

the identified hits was more stable. RMSD plot of all the systems, the control system and the Apo state is displayed in Figure 4.

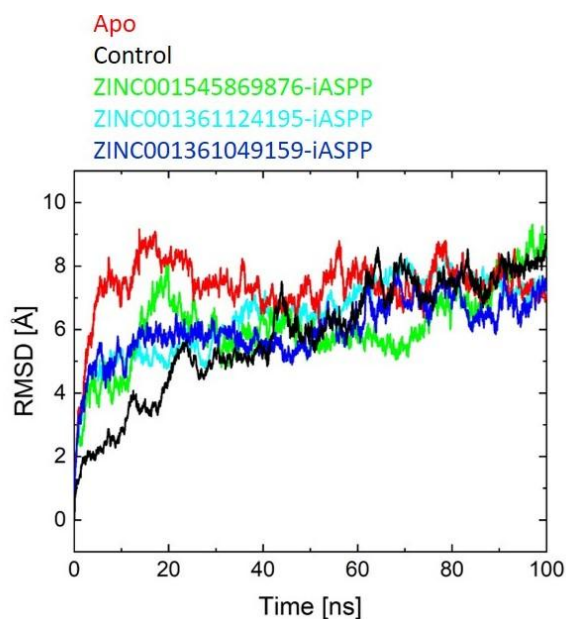


Figure 4. RMSD plots for ZINC001361124195-iASPP (Cyan), ZINC001361049159-iASPP (Blue), ZINC001545869876-iASPP (Green), Control (Black) and Apo-state (Red).

3.4.2 Residue Flexibility Index Analysis

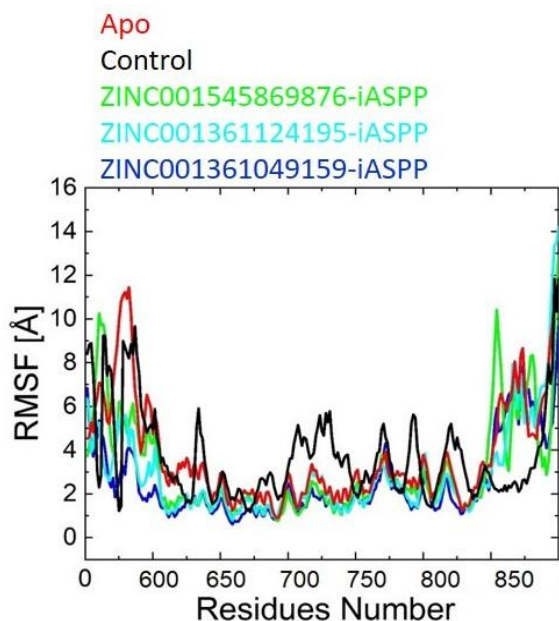


Figure 5. RMSF plots for ZINC001361124195-iASPP (Cyan), ZINC001361049159-iASPP (Blue), ZINC001545869876-iASPP (Green), Control (Black) and Apo-state (Red).

In the present study, the residue mobility and stability for the protein-ligand complexes were estimated by RMSF analysis [30]. The RMSF graph was then plotted (Figure 5) against the number of residues corresponding to the protein. The residues such as 640-648 and 801-823 revealed an unstable behavior. High fluctuations were observed in the Apo-state and the control system as compared to other systems. The residues Phe815, Gly816, Leu817, Phe818, Pro819, Arg820, Val821, Lys822 and

Pro823 revealed high flexibility. The flexible regions were mainly the loop regions. The active site residues including PHE720, THR722, THR729, PHE731, GLU732, GLU752, GLN753, ARG790, ASP791, PRO793, ASP797, and TRP799 indicates less fluctuation. The RMSF plot for all the systems is shown in Figure 5.

3.4.3 Structure Compactness Analysis

During the simulation, the Rg revealed the overall compactness of the protein-ligand complexes. The system stability is calculated by a moderately lower change in Rg, which is also a sign of a stable folded protein structure [31]. The ZINC001361049159-iASPP complex is more tightly packed, as evidenced by the Figure 6. The mean Rg value of the ZINC001361049159-iASPP complex was found to be 19.5-19.8 Å while that of the ZINC001361124195-iASPP complex was observed to be 19.4-21.0 Å. The Rg value of the ZINC001545869876-iASPP complex was found to be 20.5-23.5 Å. As compared protein-ligand complexes the Rg value of the Apo state was very high. The mean Rg of the Apo state was observed to be 20.1-24.4 Å.

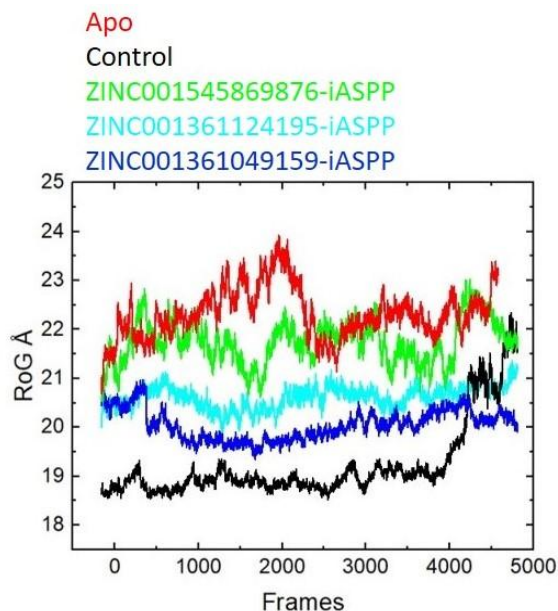


Figure 6. Rg plots for ZINC001361124195-iASPP (Cyan), ZINC001361049159-iASPP (Blue), ZINC001545869876-iASPP (Green), Control (Black) and Apo-state (Red).

3.4.4 Dynamics Cross-Correlation Map (DCCM)

The positive and negative correlations of the amino acid can be shown in the dynamical cross-correlation analysis. DCCM exhibited an overall correlation that was between -1.0 and +1.0. The degree of relationship between residues was shown by different colors, with deeper green signifying stronger associations. DCCM analysis revealed that more positive correlations were observed in the ZINC001361049159-iASPP and ZINC001361124195-iASPP complexes while more negative correlations were observed in the ZINC001545869876-iASPP and Apo-state. Figure 7 displays the DCCM plot for all the complexes as well as the control complex. The final snapshots after 100 ns MD simulation are shown in Figure 8.

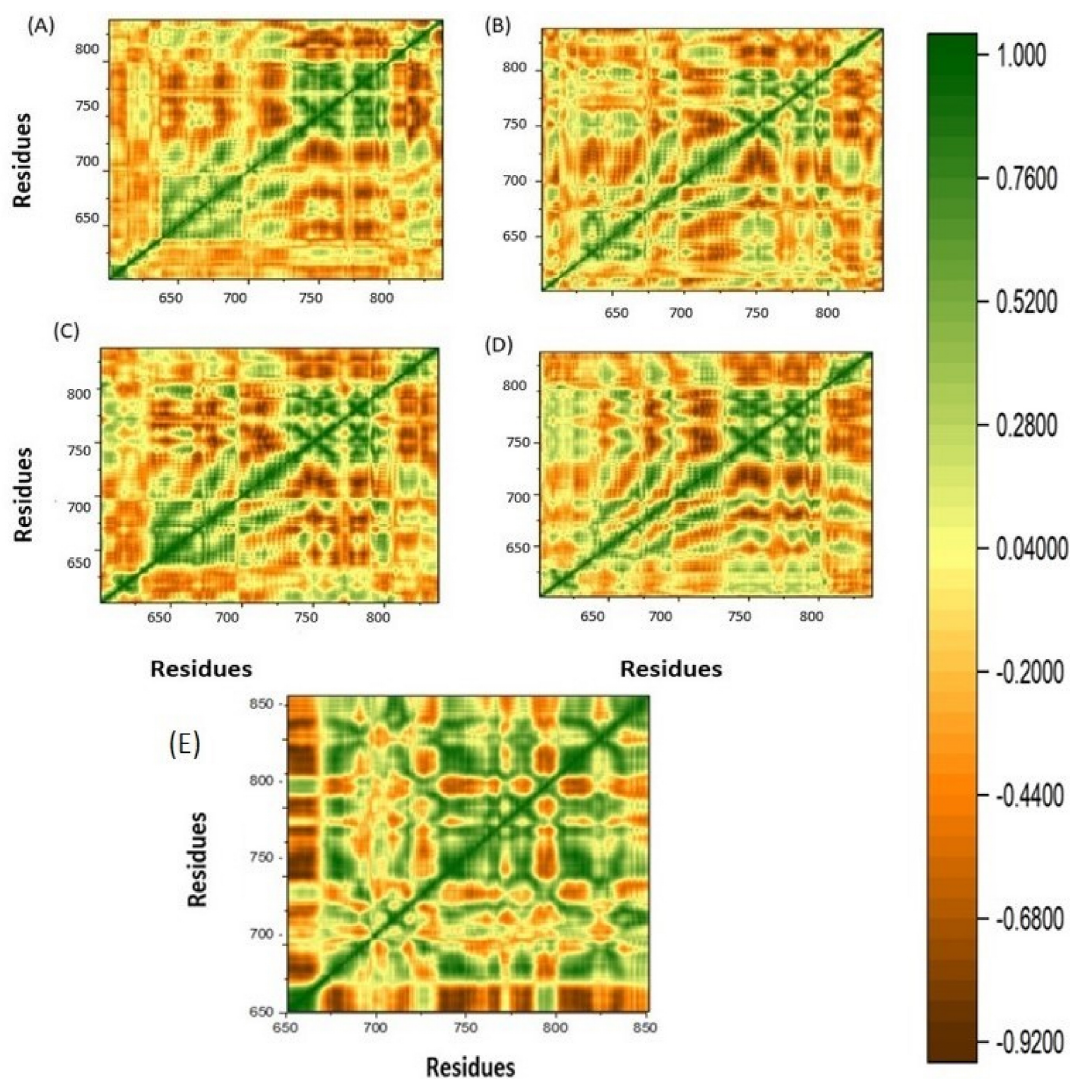


Figure 7. DCCM plots for (A) ZINC001361049159-iASPP (B) ZINC001361124195-iASPP (C) ZINC001545869876-iASPP, (D) Apo-state and (E) Control complex.

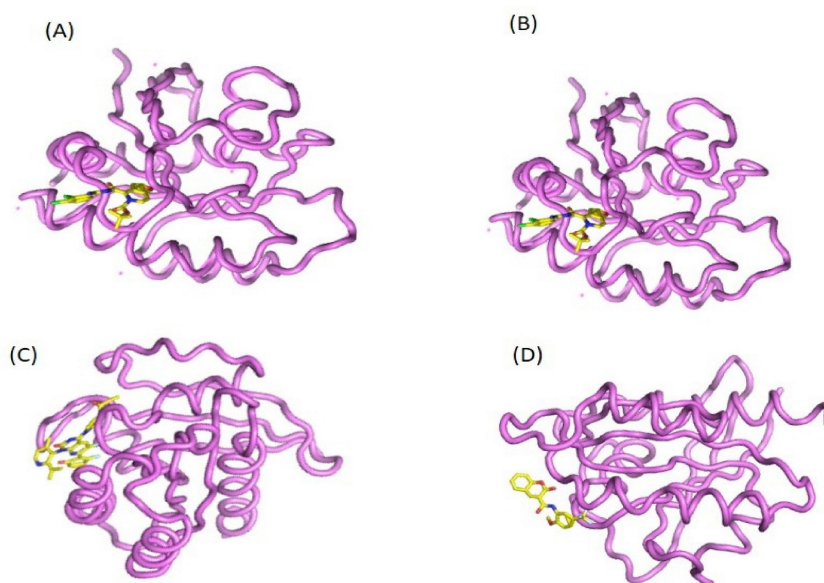


Figure 8. Snapshots of 100 ns MD simulation (A) ZINC001361124195-iASPP, (B) ZINC001361049159-iASPP, (C) ZINC001545869876-iASPP and (D) Control

3.5 MMGBSA Analysis

Table 4 shows the results of the MMGBSA analysis. The MMGBSA analysis shows that the compound ZINC001361049159 has a high affinity for the iASPP receptor. The total binding energy (ΔG) value for the ZINC001361049159-iASPP complex was found to be -

40Kcal/mol. The total energy for the ZINC001361124195-iASPP and ZINC001545869876-iASPP complexes were found as -35 and -20 Kcal/mol (Table 3). The MMGBSA analysis was in agreement with the molecular docking result. As compared to the control compound all other compounds revealed good binding free energy score.

Table 4. MMGBSA analysis for the complexes

Complexes	VDW	EEL	ESURF	EGB	ΔG Total
ZINC001361049159	-51.98	-11.82	-6.09	29.10	-40.79
ZINC001361124195	-46.23	0.54	-5.41	15.63	-35.47
ZINC001545869876	-27.22	-19.28	-2.97	29.32	-20.15
Control	-28.45	-33.29	-3.82	45.43	-20.12

4. Discussion

Cancer is a diverse and multifaceted illness where several genetic and molecular alterations lead to uncontrolled cell growth and proliferation, which quickly increases tissue mass in the affected areas of the body [32]. Over the years, an enormous number of natural anti-cancer drugs have been discovered to limit tumor growth in a variety of ways. Most of these drugs affect vital biological enzymes, while some might alter cell metabolism [33]. These drugs are selective for a variety of cancer types and have different mechanisms of action [34]. A rising number of cancer patients benefit from current cancer treatments, such as immunotherapy, targeted therapy, radiation therapy, chemotherapy, and surgery. However, drug resistance, which continues to be a major barrier to the curative treatment of a variety of malignancies, limits the effectiveness of these approaches [9]. Additional therapeutic approaches for treating many cancer types rely on the use of small molecules, such as plasmids, short RNAs, and genes. However, these approaches have drawbacks because of the poor stability of these molecules in vivo [35].

iASPP overexpression is associated with diverse human tumors [36]. One of the possible ways to restore the p53 function may be possible by targeting iASPP [10]. Virtual screening (VS) has been described as a significant alternative to traditional HTS campaigns [37]. Because actual positive hit rates with VS are typically significantly greater than those with "random" testing procedures [38]. Pharmacophore-based virtual screening (VS) is extensively used in various stages of the drug development process. Although reported hit rates from virtual screening differ from study to study, they usually fall between 5% and 40%. Conversely, the hit rates for identifying active molecules are usually less than 1% upon random testing of compounds [39]. Previously, several studies used Pharmacophore modeling to identify new inhibitors against different drug targets. For instance, Huma et al. used Pharmacophore modeling and identified compounds against STAT3 a cancer drug target [40]. Here, we employed virtual screening based on the Pharmacophore model for the prediction of new hits against iASPP drug target. We retrieved 12000 drug-like molecules from the ZINC database for the virtual screening purpose. A pharmacophore model was generated and validated by the GH scoring method. The

validated model predicts 36/12000 active compounds against the iASPP cancer drug target. Most of the compounds displayed strong interactions with iASPP. To confirm the stability of the compounds the top 03 best docking scores compounds were subjected to MD simulation and the result was compared with the Apo state. Post-simulation analysis including RMSD, RMSF, RoG and DCCM analysis revealed that the compounds ZINC001361049159, ZINC001361124195, and ZINC001545869876 formed stable complexes with the iASPP receptor. The MMGBSA analysis also confirmed that the compounds ZINC001361049159, ZINC001361124195, and ZINC001545869876 displayed strong affinity towards the iASPP receptor.

5. Conclusion

In conclusion, an extensive method including pharmacophore modeling, molecular docking, and MD simulation has been effectively applied. Thirty-six hit compounds were obtained as a result of the virtual screening procedure. The hits revealed a strong binding affinity for the iASPP target. Compounds ZINC001361049159, ZINC001361124195, and ZINC001545869876 were highly stable. Furthermore, the findings indicate that the screening technique exhibits significant promise in predicting strong inhibitors of the iASPP target. In the future, this integrated procedure may likely be applied to other members of the P53 family of proteins. Pharmacophore-based virtual screening offers inexpensive screening of databases. One of the major limitations of this study is the lack of experimental validation of the identified compounds.

Acknowledgments

The authors thank Dr. Ajmal Khan, University of Nizwa for providing technical support for the computational study.

Conflicts of Interest

The authors have no conflict of interest.

Author Contribution

Conceptualization: AW and SA

Methodology: AA, MJ, MFA, SA, MR and SH

Software: MJ and AW

Validation: MR and MFA

Formal analysis: SH

Investigation: AA and MFA

Resources: MJ and SA

Data curation: MR and SH

Writing—original draft preparation: AA and AW

Writing—review and editing: MJ, MFA, SA, MR, SH and AW

Visualization, AA and SA

Supervision, SA and AW

Project administration: MR and AW

All authors have read and agreed to the published version of the manuscript.

References

- [1] Siegel RL, Miller KD, Jemal A. Cancer statistics, 2018. *A Cancer Journal for Clinicians*. 2018, 68, 7-30. DOI: 10.3322/caac.21442
- [2] Jia Y, Yun CH, Park E, Ercan D, Manuia M, et al. Overcoming EGFR (T790M) and EGFR (C797S) resistance with mutant-selective allosteric inhibitors. *Nature*. 2016, 534, 129-32. DOI: 10.1038/nature17960
- [3] Shi D, Gu W. Dual roles of MDM2 in the regulation of p53: ubiquitination dependent and ubiquitination independent mechanisms of MDM2 repression of p53 activity. *Genes & Cancer*. 2012, 3, 240-8. DOI: 10.1177/1947601912455199
- [4] Olivier M, Hollstein M, Hainaut P. TP53 mutations in human cancers: origins, consequences, and clinical use. *Cold Spring Harbor Perspectives in Biology*. 2010, 2, a001008. DOI: 10.1101/cshperspect.a001008
- [5] Muller PA, Vousden KH. p53 mutations in cancer. *Nature Cell Biology*. 2013, 15, 2-8. DOI: 10.1038/ncb2641
- [6] Biegging KT, Mello SS, Attardi LD. Unravelling mechanisms of p53-mediated tumour suppression. *Nature Reviews Cancer*. 2014, 14, 359-70. DOI: 10.1038/nrc3711
- [7] Liu Z, Zhang X, Huang D, Liu Y, Zhang X, et al. Elevated expression of iASPP in head and neck squamous cell carcinoma and its clinical significance. *Medical Oncology*. 2012, 29, 3381-8. DOI: 10.1007/s12032-012-0306-9
- [8] Cai Y, Qiu S, Gao X, Gu SZ, Liu ZJ. iASPP inhibits p53-independent apoptosis by inhibiting transcriptional activity of p63/p73 on promoters of proapoptotic genes. *Apoptosis*. 2012, 17, 777-83. DOI: 10.1007/s10495-012-0728-z
- [9] Dong P, Ihira K, Hamada J, Watari H, Yamada T, et al. Reactivating p53 functions by suppressing its novel inhibitor iASPP: a potential therapeutic opportunity in p53 wild-type tumors. *Oncotarget*. 2015, 6, 19968. DOI: 10.18632/oncotarget.4847
- [10] Qiu S, Cai Y, Gao X, Gu SZ, Liu ZJ. A small peptide derived from p53 linker region can resume the apoptotic activity of p53 by sequestering iASPP with p53. *Cancer Letters*. 2015, 356, 910-7. DOI: 10.1016/j.canlet.2014.10.044
- [11] Sertkaya A, Beleche T, Jessup A, Sommers BD. Costs of drug development and research and development intensity in the US, 2000-2018. *JAMA Network Open*. 2024, 7(6), e2415445. DOI: 10.1001/jamanetworkopen.2024.15445
- [12] Ece A. Computer-aided drug design. *BMC Chemistry*. 2023, 17, 26. DOI: 10.1186/s13065-023-00939-w
- [13] Zhou Y, Tang S, Chen T, Niu MM. Structure-based pharmacophore modeling, virtual screening, molecular docking and biological evaluation for identification of potential poly (ADP-Ribose) polymerase-1 (PARP-1) inhibitors. *Molecules*. 2019, 24, 4258. DOI: 10.3390/molecules24234258
- [14] Ramírez D, Concha G, Arévalo B, Prent-Peñaloza L, Zúñiga L, et al. Discovery of novel TASK-3 channel blockers using a pharmacophore-based virtual screening. *International Journal of Molecular Sciences*. 2019, 20, 4014. DOI: 10.3390/ijms20164014
- [15] Chen S, Wu J, Zhong S, Li Y, Zhang P, et al. iASPP mediates p53 selectivity through a modular mechanism fine-tuning DNA recognition. *Proceedings of the National Academy of Sciences*. 2019, 116, 17470-9. DOI: 10.1073/pnas.1909393116
- [16] Wadood A, Ghufuran M, Hassan SF, Khan H, Azam SS, et al. In silico identification of promiscuous scaffolds as potential inhibitors of 1-deoxy-d-xylulose 5-phosphate reductoisomerase for treatment of Falciparum malaria. *Pharmaceutical Biology*. 2017, 55, 19-32. DOI: 10.1080/13880209.2016.1225778
- [17] Li RJ, Wang YL, Wang QH, Wang J, Cheng MS. In Silico Design of Human IMPDH Inhibitors Using Pharmacophore Mapping and Molecular Docking Approaches. *Computational and Mathematical Methods in Medicine*. 2015, 418767. DOI: 10.1155/2015/418767
- [18] El-Hasab MAE-M, El-Bastawissy EE, El-Moselhy TF. Identification of potential inhibitors for HCV NS3 genotype 4a by combining protein–ligand interaction fingerprint, 3D pharmacophore, docking, and dynamic simulation. *Journal of Biomolecular Structure and Dynamics*. 2018, 36, 1713-27. DOI: 10.1080/07391102.2017.1332689
- [19] Wadood A, Jamal SB, Riaz M, Mir A. Computational analysis of benzofuran-2-carboxylic acids as potent Pim-1 kinase inhibitors. *Pharmaceutical Biology*. 2014, 52, 1170-8. DOI: 10.3109/13880209.2014.880488
- [20] Wadood A, Khan H, Ghufuran M, Hassan H, Shams S, et al. Structure-Based Development of New and Potent Inhibitors of PIM Kinases: A Computational Study. *Journal of the Chemical Society of Pakistan*. 2017, 39.
- [21] Karthikeyan M, Vyas R. Active Site-Directed Pose Prediction Programs for Efficient Filtering of Molecules. In: Karthikeyan M, Vyas R (eds). *Practical Chemoinformatics*. 2014, 271-316. DOI: 10.1007/978-81-322-1780-0_5
- [22] Wadood A, Ulhaq Z. In silico identification of novel inhibitors against Plasmodium falciparum dihydroorotate dehydrogenase. *Journal of Molecular Graphics and Modelling*. 2013, 40, 40-7. DOI: 10.1016/j.jmgm.2012.11.010
- [23] Hussein D, Saka M, Baeesa S, Bangash M, Alghamdi F, et al. Structure-based virtual screening and molecular docking approaches to identify potential inhibitors against KIF2C to combat glioma. *Journal of Biomolecular Structure and Dynamics*. (online ahead of print 20231109;doi:10.1080/07391102.2023.2278750), 2023, 1-14. DOI: 10.1080/07391102.2023.2278750
- [24] Wadood A, Ajmal A, Junaid M, Rehman AU, Uddin R, et al. Machine learning-based virtual screening for STAT3 anticancer drug target. *Current Pharmaceutical Design*.

- 2022, 28, 3023-32. DOI: 10.2174/1381612828666220728120523
- [25] Ajmal A, Ali Y, Khan A, Wadood A, Rehman AU. Identification of novel peptide inhibitors for the KRas-G12C variant to prevent oncogenic signaling. *Journal of Biomolecular Structure and Dynamics*. 2023, 41, 8866-75. DOI: 10.1080/07391102.2022.2138550
- [26] Junaid M, Khan MT, Malik SI, Wei DQ. Insights into the mechanisms of the pyrazinamide resistance of three pyrazinamidase mutants N11K, P69T, and D126N. *Journal of Chemical Information and Modeling*. 2018, 59, 498-508. DOI: 10.1021/acs.jcim.8b00525
- [27] Ahmad S, Khan M, Alam A, Ajmal A, Wadood A, et al. Novel flurbiprofen clubbed oxadiazole derivatives as potential urease inhibitors and their molecular docking study. *RSC Advances*. 2023, 13, 25717-28. DOI: 10.1039/d3ra03841f
- [28] Zhang S, Zhou L, El-Deiry WS. Small-molecule NSC59984 induces mutant p53 degradation through a ROS-ERK2-MDM2 Axis in cancer cells. *Molecular Cancer Research*. 2022, 20, 622-36. DOI: 10.1158/1541-7786.MCR-21-0149
- [29] Ajmal A, Mahmood A, Hayat C, Hakami MA, Alotaibi BS, et al. Computer-assisted drug repurposing for thymidylate kinase drug target in monkeypox virus. *Frontiers in Cellular and Infection Microbiology*. 2023, 13, 1159389. DOI: 10.3389/fcimb.2023.1159389
- [30] Khan A, Junaid M, Li CD, Saleem S, Humayun F, et al. Dynamics insights into the gain of flexibility by Helix-12 in ESR1 as a mechanism of resistance to drugs in breast cancer cell lines. *Frontiers in Molecular Biosciences*. 2020, 6, 159. DOI: 10.3389/fmolb.2019.00159
- [31] Junaid M, Shah M, Khan A, Li CD, Khan MT, et al. Structural-dynamic insights into the H. pylori cytotoxin-associated gene A (CagA) and its abrogation to interact with the tumor suppressor protein ASPP2 using decoy peptides. *Journal of Biomolecular Structure and Dynamics*. 2019, 37, 4035-50. DOI: 10.1080/07391102.2018.1537895
- [32] Laplagne C, Domagala M, Le Naour A, Quemerais C, Hamel D, et al. Latest advances in targeting the tumor microenvironment for tumor suppression. *International Journal of Molecular Sciences*. 2019, 20, 4719. DOI: 10.3390/ijms20194719
- [33] Bedoui S, Herold MJ, Strasser A. Emerging connectivity of programmed cell death pathways and its physiological implications. *Nature Reviews Molecular Cell Biology*. 2020, 21, 678-95. DOI: 10.1038/s41580-020-0270-8
- [34] Anand U, Dey A, Chandel AKS, Sanyal R, Mishra A, et al. Cancer chemotherapy and beyond: Current status, drug candidates, associated risks and progress in targeted therapeutics. *Genes & Diseases*. 2023, 10, 1367-401. DOI: 10.1016/j.gendis.2022.02.007
- [35] Ioele G, Chieffallo M, Occhiuzzi MA, De Luca M, Garofalo A, et al. Anticancer drugs: recent strategies to improve stability profile, pharmacokinetic and pharmacodynamic properties. *Molecules*. 2022, 27, 5436. DOI: 10.3390/molecules27175436
- [36] Lu S, Li Y, Zhu C, Wang W, Zhou Y. Managing cancer drug resistance from the perspective of inflammation. *Journal of Oncology*. 2022, 2022, 3426407. DOI: 10.1155/2022/3426407
- [37] Tanrikulu Y, Krüger B, Proschak E. The holistic integration of virtual screening in drug discovery. *Drug Discovery Today*. 2013, 18, 358-64. DOI: 10.1016/j.drudis.2013.01.007
- [38] Schuster D, Spetea M, Music M, Rief S, Fink M, et al. Morphinans and isoquinolines: acetylcholinesterase inhibition, pharmacophore modeling, and interaction with opioid receptors. *Bioorganic & Medicinal Chemistry*. 2010, 18, 5071-80. DOI: 10.1016/j.bmc.2010.05.071
- [39] Vuorinen A, Schuster D. Methods for generating and applying pharmacophore models as virtual screening filters and for bioactivity profiling. *Methods*. 2015, 71, 113-34. DOI: 10.1016/j.ymeth.2014.10.013
- [40] Rafiq H, Hu J, Hakami MA, Hazazi A, Alamri MA, et al. Identification of novel STAT3 inhibitors for liver fibrosis, using pharmacophore-based virtual screening, molecular docking, and biomolecular dynamics simulations. *Scientific Reports*. 2023, 13, 20147. DOI: 10.1038/s41598-023-461913-x